PROTEINS: Structure, Function, and Genetics 53:273–281 (2003)

Insight Into the Stability of the Hydrophobic Binding Proteins of *Escherichia coli:* Assessing the Proteins for Use as Biosensors

Branka Salopek-Sondi, Matthew C. Skeels, Derrick Swartz, and Linda A. Luck*
Department of Chemistry, Clarkson University, Potsdam, New York

ABSTRACT **Spectroscopic methods were used to monitor the unfolding of the leucine specific (LS) and the leucine-isoleucine-valine (LIV) binding proteins. Our studies indicate that ligand-free protein undergoes a simple two-state unfolding, whereas the protein-ligand complex undergoes a three-state unfolding model. Ligand binding causes significant stabilization of both proteins. There is correlation between ligand hydrophobicity and protein stabilization: the most hydrophobic ligand, isoleucine, causes the most significant stabilization of LIV protein. A disulfide bond present in N-domain of both proteins makes a large contribution to the protein stability of these periplasmic binding receptors. Proteins 2003;53:273–281.** © 2003 Wiley-Liss, Inc.

Key words: leucine-specific binding proteins; leucine-isoleucine-valine binding proteins; proteins stability

INTRODUCTION

The potential use of periplasmic binding proteins as biosensors has come to light because of their ability to reversibly bind a variety of small ligands such as sugars, amino acids, and inorganic ions. These proteins comprise a large family of functionally similar proteins with a hinge cleft binding mode for substrates. The soluble, monomeric proteins located in the space between the cell walls of gram-negative bacteria serve to function as an escort in the high-affinity active transport systems or they are initial receptors in chemosensory pathways.[1,2] The mechanism by which these proteins function in transport and signaling involves ligand binding in a pocket between the two domains and subsequent global conformational change.[3–6] This structural change allows recognition of the substrate-loaded receptor by the membrane components in either system. Key to these interactions is the stability of the receptor-ligand complex. Bound substrate lifetimes must be substantial to allow the receptor to diffuse long distances in the activated conformation in search of a docking site. Once docked to the membrane components, rapid release of ligand into the assembly expedites the addition of the nutrient to the cytoplasm. Hence, the stabilizing factors for the ligand-protein complex need to be tight enough to hold the complex together but flexible enough to release the substrate on demand. These two properties of the periplasmic binding proteins allow them to be extraordinary candidates for regeneratable biosensors.

Our laboratory is interested in the use of these periplasmic binding proteins from *E. coli*, which have the capability of being used as biosensors for small substrates. We focus this article on the hydrophobic amino acid receptors, the leucine-specific receptor (LS) and the leucine-isoleucine-valine receptor (LIV) for several reasons. First, there is a curiosity for the reason why there are two proteins associated with the transport system. They are 80% identical in amino acid content but have differing specificities for hydrophobic amino acids. These two proteins could provide a scaffold on which to mutagenize a binding pocket for a specific hydrophobic ligand. Second, our laboratory has found the leucine-specific protein is not so specific; it sequesters phenylalanine and other fluorinated compounds.[7,8] This increases the likelihood that the binding site may be altered to accommodate small molecules used in biological warfare. Hence, our biological system may be ideal for the development of biosensors. Third, these proteins have been used as models for a number of neuroreceptors including the metabotropic glutamate receptor and the N-methyl-D-aspartate receptor.[9–12] Insight into the function of the bacterial receptors will directly impact the study of Eukaryotic receptors for neurological signaling.

In this article we address the stability of the two hydrophobic amino acid receptors from *E. coli*. With use of UV and intrinsic tryptophan fluorescence we have monitored the urea denaturation of each receptor with and without ligand. Using a two-state or three-state model we have obtained thermodynamic parameters of unfolding. The stabilizing function of the disulfide bond is discussed. Understanding the structure and functionality of the receptors are needed for the development of the biotechnological applications of these proteins.

Grant sponsor: Petroleum Research Fund; Grant number: ACS-PRF#36825-AC4; Grant sponsor: National Institutes of Health; Grant number: R03-CA 89705-01; Grant sponsor: National Science Foundation: Grant number: DUE-9979509.

Branka Salopek-Sondi's present address is Rudjer Bošković Institute, Zagreb, Croatia.

*Correspondence to: Dr. Linda A. Luck, Department of Chemistry, Clarkson University, Potsdam, NY 13699. E-mail: luckla@clarkson.edu

Received 12 February 2003; Accepted 11 April 2003

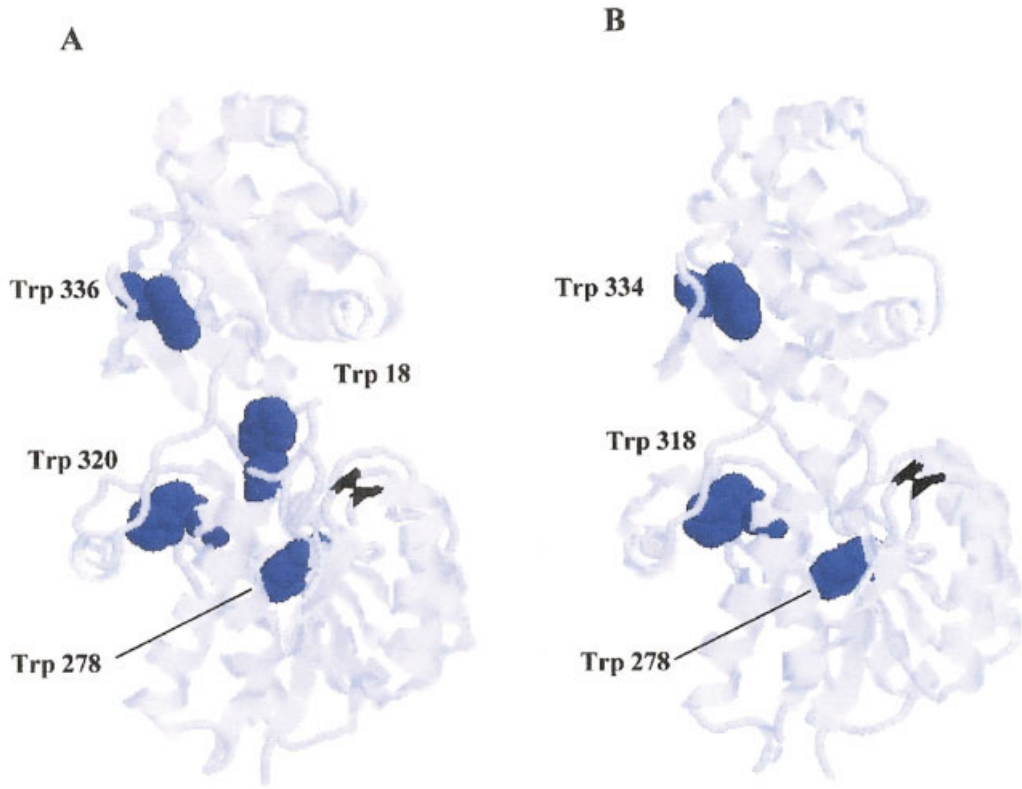

Fig. 1. Model of LS (**A**) and LIV (**B**) with space-filled highlighted intrinsic tryptophan probes. Shown is a disulfide bond between Cys 53 and Cys 78 in both proteins. Models were created from crystallographic data[28,29] using RasMol.[30]

MATERIALS AND METHODS

The strategy for production and purification of protein using the pKSty and pJSty expression plasmids[13] for LS and LIV has already been described.[7,8,14]

The urea denaturation experiments were described previously in detail.[7,15] To test the reversibility of protein unfolding, two aliquots of protein were placed into 5 M urea. One was then diluted 10-fold in 5 M urea to retain the unfolded state of the protein. The other was diluted 10-fold in 20 mM Tris-Cl buffer (pH 7.1) to promote refolding of the previously unfolded protein. These samples were monitored by fluorescence. To ensure the fluorescence change was due to the difference in concentration and not dilution, a control was also used. For this experiment, protein was added to 20 mM Tris-Cl buffer and diluted 10-fold into the same buffer.

To determine the impact of the single disulfide bond on protein stability, urea-unfolding experiments were performed in the presence of 20 mM dithiothretiol (DTT) (Sigma). Figure 1 illustrates the position of the single disulfide bond in the N-domains of both LS and LIV proteins between Cys53 and Cys78.

All fluorescence measurements were conducted at ambient temperature (25°C) by using a Perkin-Elmer LS 50B Luminescence Spectrophotometer (Norwalk, CT). The excitation and emission bandwidth was set to 5 nm. The samples were irradiated at 280 nm, and the emission was monitored from 310 to 390 nm.

To analyze our fluorescence data, we used a two-state model for the unliganded protein and a three-state model for the liganded protein. In a two-state model, equilibrium exists between the native (N) and denatured (D) states of the protein, and only N and D populate the transition region. For a two-state model, the following equation can be applied:

$$N \rightleftharpoons D \tag{1}$$

To analyze two-state unfolding data, we followed the linear extrapolation model (LEM)[16,17] as modified according to Santoro and Bolen.[18] To superimpose data from fluorescence denaturation curves, the fluorescence intensities were converted into values corresponding to fractions of unfolded peptides. In cases where a stable intermediate can be detected in the unfolding transition, a three-state unfolding model can be used to describe the transition

$$N \rightleftharpoons I \rightleftharpoons D \tag{2}$$

where N, I, and D are the native, intermediate, and denatured states, respectively. A nonlinear fitting equation for a three-state unfolding was developed after a similar analysis of Santoro and Bolen.[18] A complete descrip-

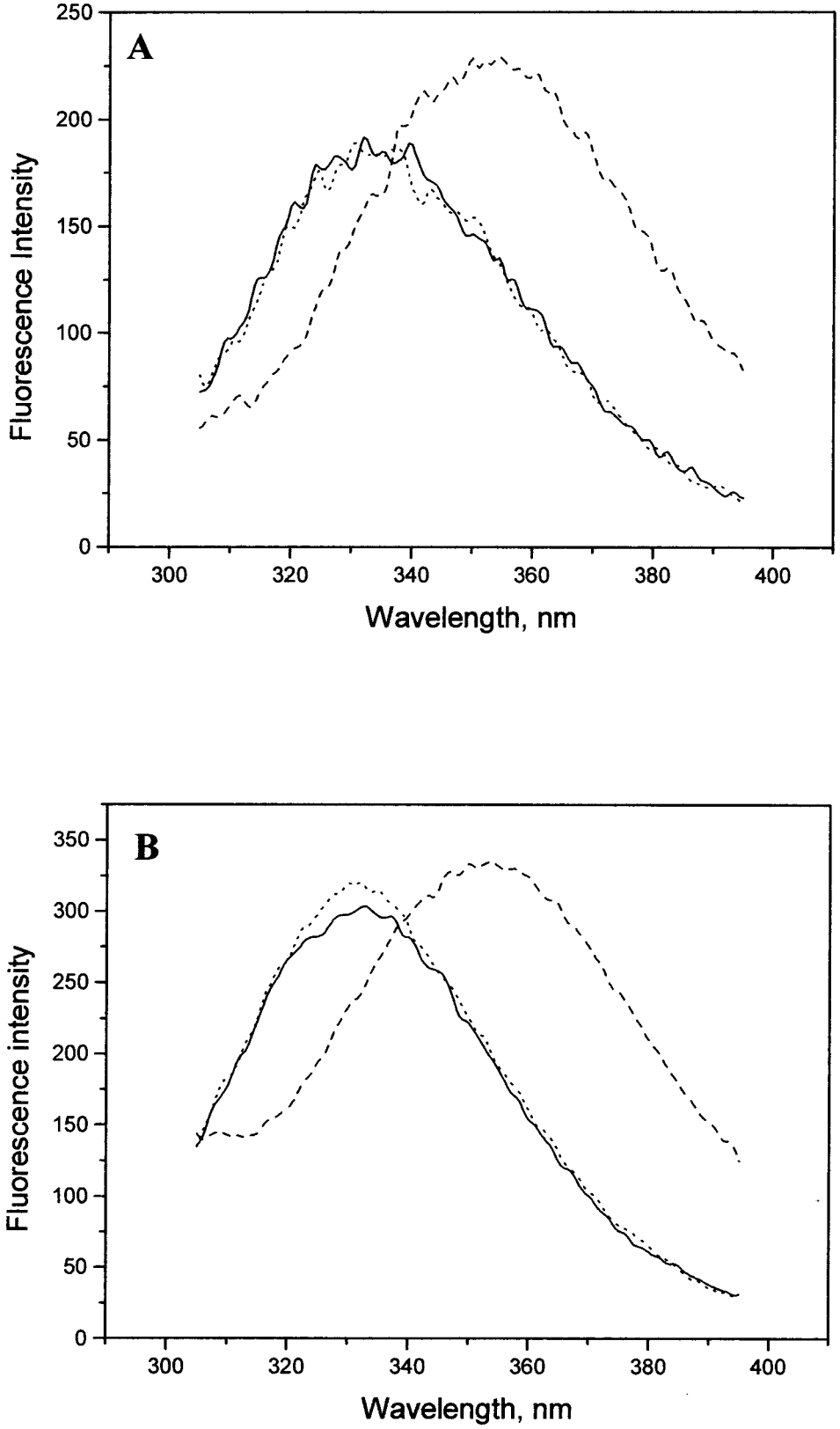

Fig. 2. Protein-folding reversibility of LS (**A**) and LIV (**B**). Bold lines represent native proteins, dashed lines represent fully unfolded protein, and dotted lines represent refolded proteins.

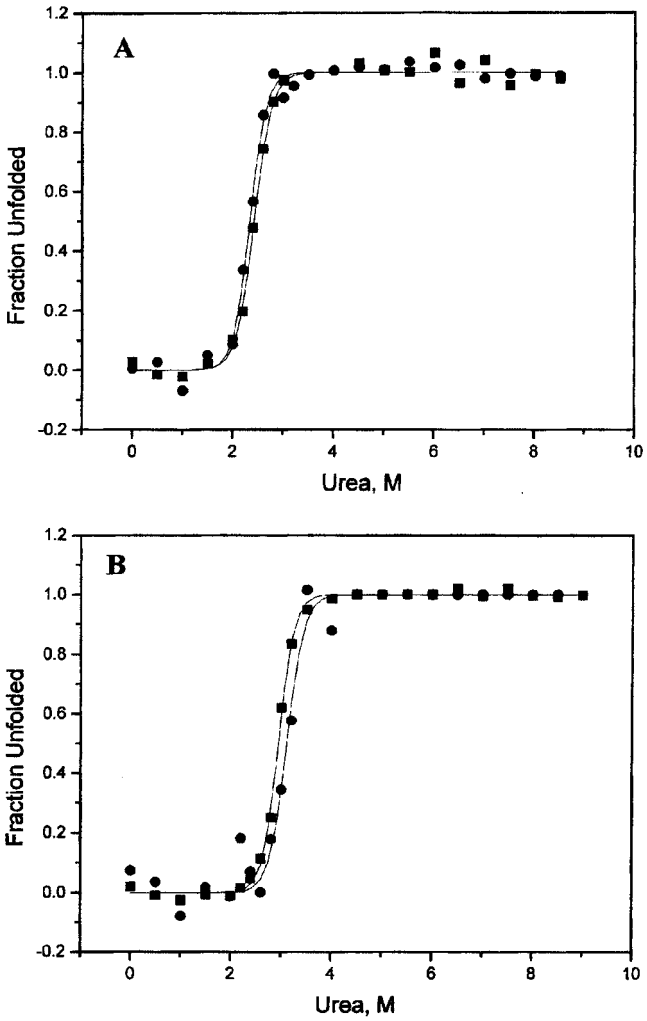

Fig. 3. Comparison of the two-state unfolding transitions of LS (**A**) and LIV (**B**) monitored by intrinsic tryptophan fluorescence (■) and by second derivative UV methods (●).

tion of the mathematics appears in the PhD thesis of Matthew Skeels.[15]

RESULTS AND DISCUSSION

LS and LIV are very similar proteins in amino acid composition and structure. However, the substrate-binding pocket differs, lending to the unique specificity of these proteins. The most striking difference between the two is position 18 located in the center of the binding pocket. In LS, this amino acid is a tryptophan, and in LIV there is a tyrosine residue. Our denaturation and thermodynamic studies use the intrinsic tryptophan residues. LS and LIV have three tryptophan residues (W278, 320, 336 in LS and W278, 318, 334 in LIV) at similar positions in the protein interior, and as mentioned above, LS possesses an additional residue (W18), located in the ligand-binding pocket. These residues, which provide valuable intrinsic probes to monitor unfolding, are illustrated in Figure 1. Two of the three congruent tryptophan residues are located in the N-terminal domain, and one is located in the C-terminal domain.

TABLE I. ΔG^{o}_{H2O} for the Unfolding of LS and LIV Proteins in the Presence of Ligand and Dithiothreitol[†]

Protein	Ligand	ΔG^{o}_{1} (kJ/mol)	ΔG^{o}_{2} (kJ/mol)	ΔG^{o}_{H2O} (kJ/mol)+/−
LS	None	—	—	34.5 ± 3.1[a]
	−, +DTT	—	—	25.3 ± 2.1
	Leucine	33.9	35.7	69.6 ± 3.6
LIV	None	—	—	33.3 ± 1.6[a]
	−, +DTT	—	—	27.4 ± 1.0
	Leucine	25.0	55.7	80.7 ± 1.4[a]
	Isoleucine	25.1	61.9	87.0 ± 1.8[a]
	Valine	25.1	52.0	77.1 ± 3.5[a]

[†]Values are calculated by two- or three- state equations appropriate to the experiment.
[a]Results were previously reported.[7]

To obtain thermodynamic parameters of unfolding, we examined the experimental conditions to ensure that the protein and ligand concentration were correct and the reversibility of the unfolding process occurred. Thermodynamic parameters from urea-induced unfolding can be derived only when the system is in equilibrium. In other words, the proteins after denaturation must refold. We tested each of the proteins to make sure this condition was met. Figure 2 illustrates the experiments in which we saw the reversible unfolding of LS (A) and LIV (B). Maximum fluorescence intensity of the proteins is shifted from 333 nm in native state to 358 nm in urea-denaturated state. After a 10-fold dilution of denaturant, refolding of previously unfolded LS and LIV proteins takes place. The refolding curve is not completely overlapping the native state curve protein because there is still the presence of 0.5 M urea in refolded protein sample. In essence, the systems are reversible.

The urea-induced denaturation of LS and LIV without bound substrate was monitored by intrinsic tryptophan fluorescence. As the urea concentration increased, there was a red shift in the emission maximum from 330 to 355 nm with a twofold change in fluorescence intensity at 323.5 nm. The single sigmoid transition in Figure 3 suggests that LS (3A) and LIV (3B) without bound ligand undergo a distinct two-state unfolding in which the native protein is in equilibrium with the unfolded protein. To corroborate this finding, we monitored the unfolding of LS and LIV by UV absorption spectroscopy, which is also shown in Figure 3. The classic method for determining if the unfolding of a protein is two-state or multistate is to monitor the unfolding with separate independent methods.[19] Under the same conditions, the UV absorption spectroscopy showed a decrease in the second derivative UV ratio. The coincidence of the unfolding transitions as monitored by intrinsic tryptophan fluorescence and with second derivative UV methods provides sufficient evidence to describe the unfolding of LS and LIV as two-state. In addition, the Gibbs free energy determined by UV method for LS and LIV were 35.9 ± 2.1 kJ/mol and 31.6 ± 1.3 kJ/mol, respectively, which are very similar to the values

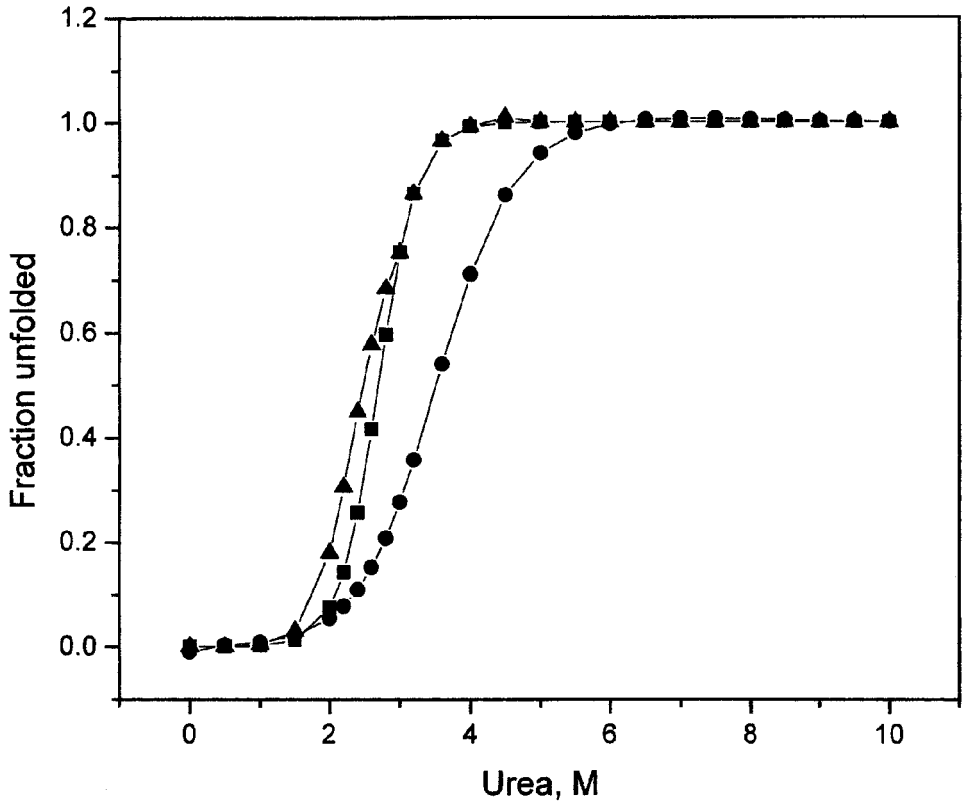

Fig. 4. Effect of protein concentration on the urea unfolding curve of LS: 5 nM (▲), 0.5 μM (■), and 50 μM (●).

obtained by intrinsic tryptophan fluorescence shown in Table I.

To ensure that the protein concentration did not affect the unfolding results due to protein–protein interactions or aggregation, we examined the denaturation of the protein at four different concentrations (5 nM, 0.5 μM, and 50 μM). The experiments are shown in Figure 4. Concentrations of protein 5 nM and 0.5 μM show similar results however; at 50 μM concentration, there is a shift in the curve to higher urea concentration. This shift in the curve leads us to believe that higher concentrations of protein cause stabilization of LS through protein–protein interactions. To disallow this phenomenon, we used a 0.5 μM protein concentration for all unfolding studies.

Urea denaturation studies with ligand showed a stabilizing effect compared with the protein without ligand as observed in Figure 5. The unfolding transition of LS and LIV with bound ligand does not follow the single sigmoid transition. There is an inflection point that suggests there is a three-state mechanism for unfolding of the protein. The protein can exist in a folded, an unfolded, and an intermediate state. To ensure that the experiments were performed with adequate amount of ligand, we monitor the effect of the ligand concentration on the protein-unfolding experiments. LS (0.5 μM) was equilibrated with 0.1 mM, 5 mM, and 50 mM L-leucine in three separate experiment, and the unfolding curves were generated. Figure 5 shows that the presence of large molar excess of ligand (5 and 50 mM) shifts the midpoint of the unfolding curve toward higher urea concentrations (from 2.7 M to 3.5 M urea) and shows an inflection of the curve, whereas 0.1 mM concentration of ligand exhibits a single sigmoid curve similar to that of the protein without ligand.

As the protein unfolds, the tertiary structure changes, which affects the ligand binding capacity. As one would expect, the partially unfolded protein has less affinity for the ligand. If one wants to maintain the ligand-bound state during the experiment, a large excess of ligand must be present. To this end, we included 5 mM concentration of ligand and 0.5 μM concentration of protein when performing all ligand-bound urea denaturation studies.

The increase resistance to urea denaturation of LS and LIV with ligands suggests that ligand binding stabilizes the proteins. The unfolding curves with protein and ligand could not be fit by a simple two-state mechanism but were fit with a three-state model for unfolding (Fig. 6).[15] The Gibbs free energy of unfolding for the LS and LIV using the three-state model with a variety of ligands is shown in Table I. Binding of leucine, a natural ligand, to both LS and LIV showed an intermediate state and an increased stability to denaturation by urea. For LS, there was an increased ΔG°_{H2O} from 34.5 kJ/mol for unliganded LS to 69.6 kJ/mol in the liganded state. To test our hypothesis that ligand binding increases stability to urea denaturation, we added an unnatural ligand glycine in the experiment. Glycine failed to stabilize LS to denaturation, and

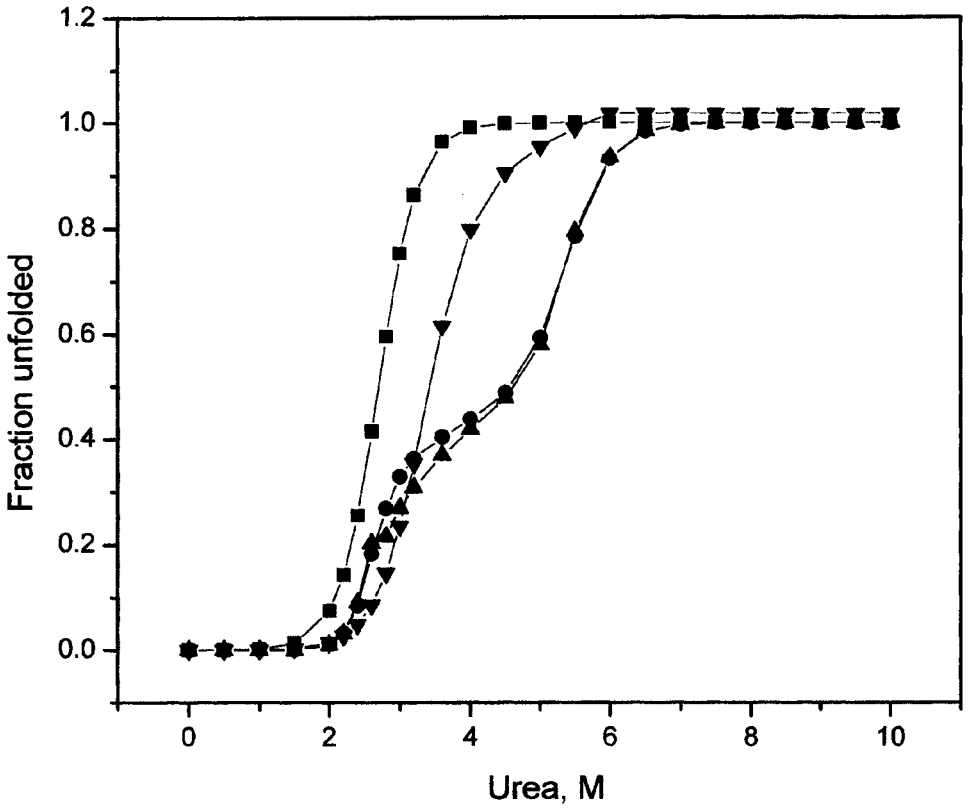

Fig. 5. Urea unfolding curve of LS protein (5 μM) without ligand (■) and saturated with L-leucine in concentration: 0.1 mM (▼), 5 mM (●), and 50 mM (▲).

the unfolding curve was identical to that of LS without ligand (results not shown).

Urea denaturation experiments with LIV with leucine or valine bound show shifts in the unfolding transition midpoint from 3.0 to 4.5 M urea, whereas the experiments with isoleucine bound show a shift in the transition midpoint to a higher urea concentration near 5.5 M. These curves are illustrated in Figure 6(B). In each case, the unfolding is clearly biphasic, containing two overlapping sigmoid transitions and following three-state unfolding models. The results of the nonlinear fitting of the unfolding transitions are given in Table I. ΔG°_{H2O} was increased from 33.3 kJ/mol for unliganded LIV to 77.1 kJ/mol, 80.7 kJ/mol, or 87.0 kJ/mol when valine, leucine, or isoleucine was bound, respectively. The most significant stabilization of LIV was caused by binding of the most hydrophobic ligand, isoleucine.

The urea-induced unfolding of LS and LIV with ligand indicate a ligand-induced stabilization of the native proteins. As seen in Figure 6, higher concentrations of urea are required to reach the unfolded state when ligand is present. In other words, the binding of ligand by the receptor results in conformation that is more stable to urea-induced unfolding than the unliganded protein. The increased stability can be attributed to the ligand-induced structural changes that take place when the substrate is held in the binding cleft through a host of forces including hydrophobic, van der Waals, and electrostatic interactions.[20] Schellman[21] predicted that ligand binding would increase the stability of a native protein by an additional amount equal to ΔG_b, which is calculated from the following equation. $\Delta G_b = RT \ln(1+K[x])$, where K is the binding constant, and [x] is the activity of the ligand. We clearly see an increase in the ΔG°_{H2O} of LIV bound to isoleucine compared to the ligands valine and leucine. The binding constant of isoleucine, the most hydrophobic of the ligands, shows highest affinity of this ligand for LIV. This could be in part due to the interactions of the ligand with the protein but could also be due to the desire for the ligand to be sequestered away from the hydrophilic solvent. Thus, the stability imparted by ligand binding may not be solely due to the electronic interactions of the ligand and protein but may be due to the driving force of the ligand to be away from a hydrophilic environment.

Based on work by Brandts et al.[22] describing models for the unfolding of proteins with interacting domains, it is possible to assume that the three-state model is a result of ligand binding to primarily one of the two domains. By studying the partially unfolded phosphoglycerate kinase (PGK), a two-domain protein, Brandts was able to determine that binding of ligand (MgATP) occurs primarily to one domain (the binding domain) and that the other domain (the regulatory domain) becomes partially bound either from ligand-domain interactions or through ligand-dependent changes in the interactions between the two domains. This mechanism may also be attributed to LS

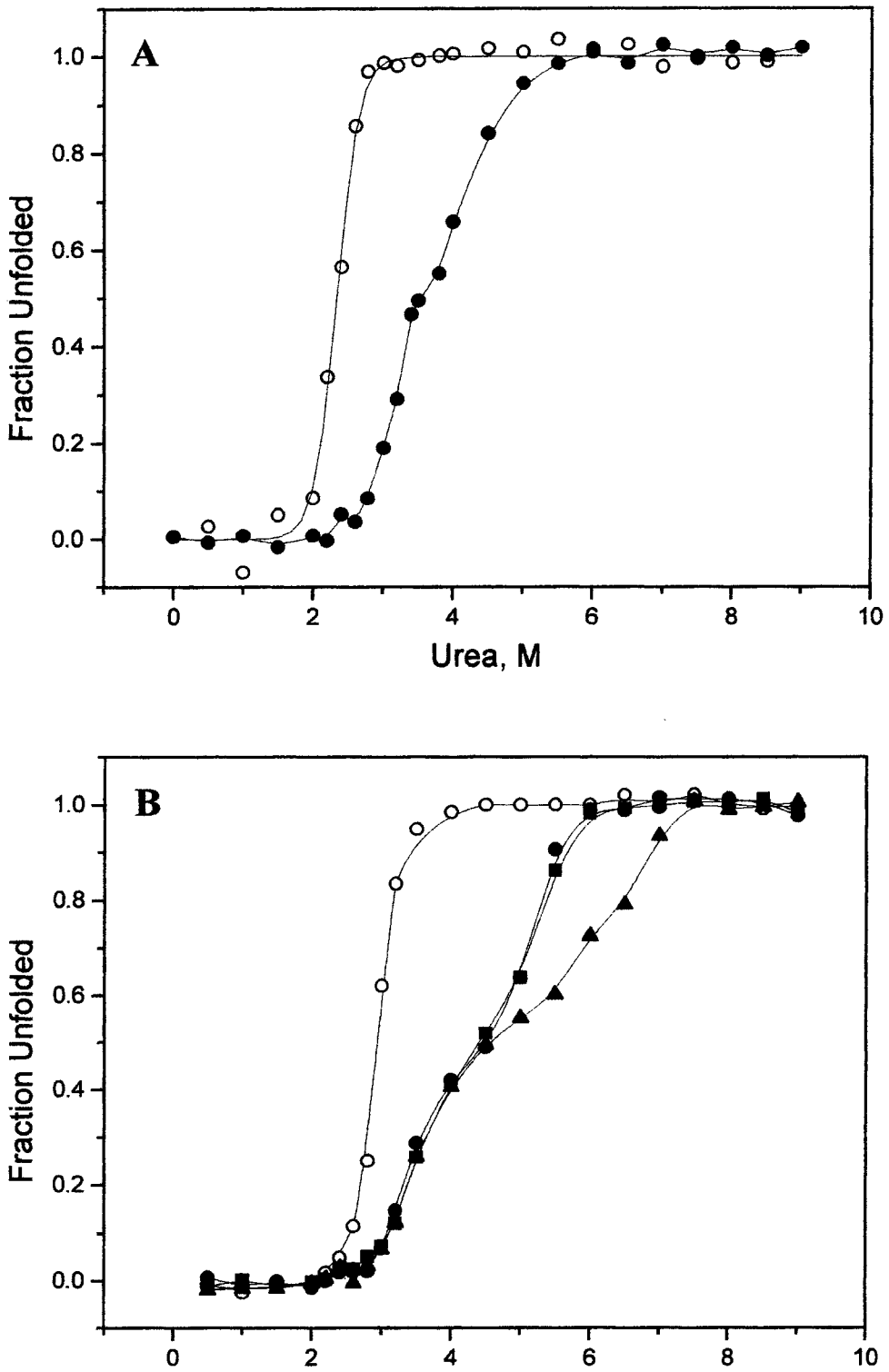

Fig. 6. Urea denaturation curve of 0.5 μM LS (**A**) and LIV (**B**) without ligand (○) and saturated with 5 mM ligand: L-leucine (●), L-isoleucine (▲), and L-valine (■).

and LIV where we observe a ligand stabilization of both domains but a preferential increase in resistance to urea denaturation of one of those domains. Ongoing mutation studies of the tryptophan residues will give us more insight as to which domain unfolds first. These studies will be the subject of another publication.

To explore the impact of disulfide bond present in N-lobe of each protein on their stability, LS and LIV proteins

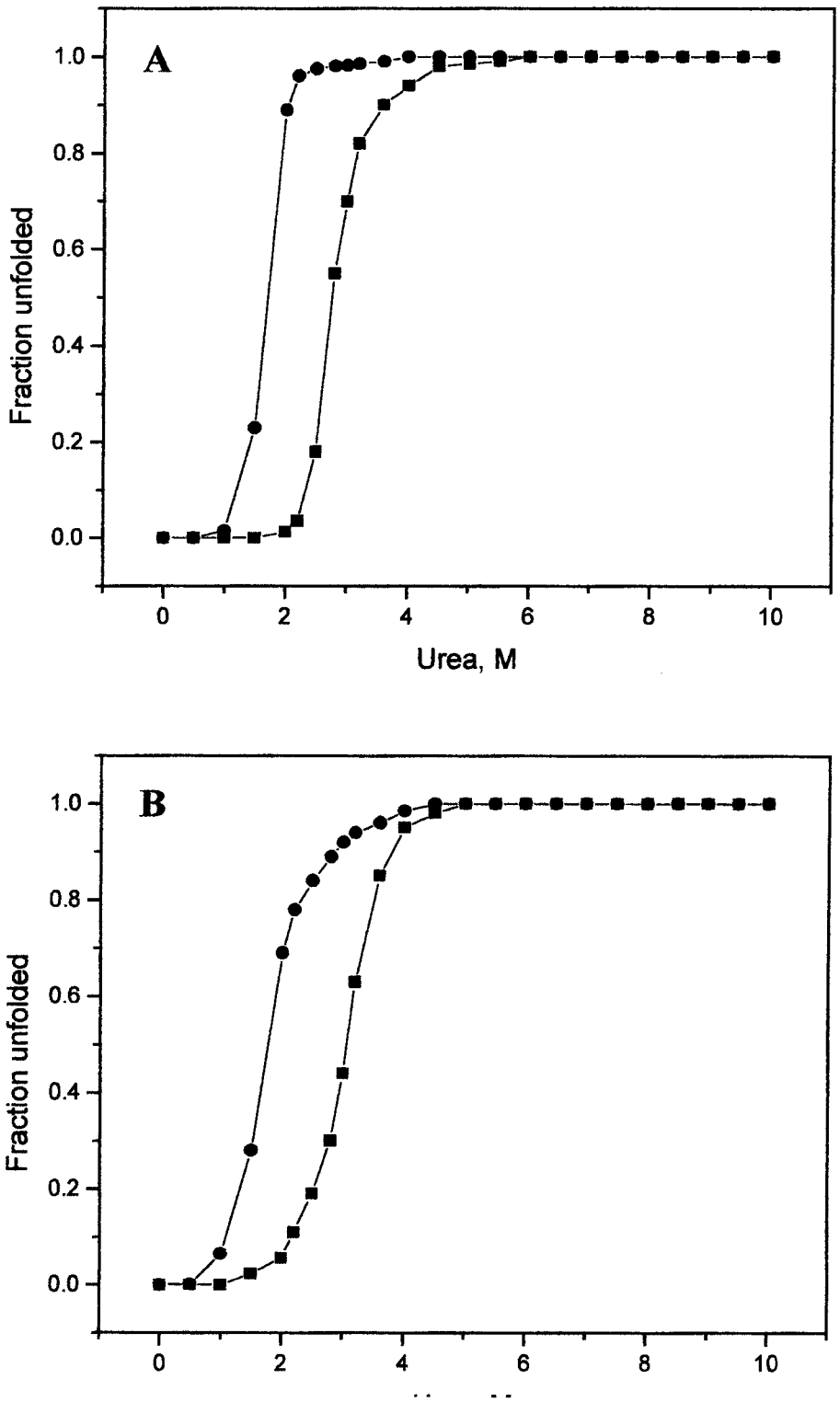

Fig. 7. The effect of DTT on the stability of LS and LIV. LS (**A**) and LIV (**B**) without ligand and without DTT are represented by the filled squares (■). The experiment with DTT added is represented by the filled circles (●)

without ligand were incubated with 20 mM DTT, and urea denaturation was performed. Figure 7 shows the unfolding curve that illustrates a decrease of stability in both proteins when the disulfide bond was reduced. ΔG°_{H2O} of unfolding was decreased in LS and LIV proteins approximately 27% and 18%, respectively (Table I). Results sug-

gest that the single disulfide bond makes a significant contribution to the stability of both proteins. It is well known from literature that disulfide bonds play a unique role in stabilizing the proteins by providing a cross-link between segments of the polypeptide chains.[23–25] It has been suggested that the major contribution of disulfide bond stability is related to a decrease in the conformational chain entropy.[26,27] Clearly, the role of this disulfide bond is to stabilize the N-terminal domain of these proteins. Care must be taken to preserve this bond when using these proteins for biosensors.

ACKNOWLEDGMENTS

The authors thank Dr. Dale Oxender for donating the vector harboring the genes for LS and LIV proteins. Funding for Derrick Swartz was provided by the National Science Foundation through a K-12 Fellowship.

REFERENCES

1. Adams MD, Oxender DL. Bacterial periplasmic binding protein tertiary structures. J Biol Chem 1989;264:15739–15742.
2. Quiocho FA, Ledvina PS. Atomic structure and specificity of bacterial periplasmic receptors for active transport and chemotaxis: variation of common themes. Mol Microbiol 1996;20:17–25.
3. Shilton BH, Flocco MM, Nilsson M, Mowbray SL. Conformational changes of three periplasmic receptors for bacterial chemotaxis and transport: the maltose-, glucose/galactose- and ribose-binding proteins. J Mol Biol 1996;264:350–363.
4. Mowbray SL Bacterial chemoreceptors: recent progress in structure and function. Mol Cells 1999;9:115–118.
5. Luck LA, Falke JJ. Open conformation of a substrate-binding cleft: ^{19}F NMR studies of cleft angle in the D-galactose chemosensory receptor. Biochemistry 1991;30:6484–6490.
6. Luck LA, Falke JJ. ^{19}F NMR studies of the D-galactose chemosensory receptor. 1. Sugar binding yields a global structural change. Biochemistry 1991;30:4248–4256.
7. Salopek-Sondi B, Swartz D, Adams PS, Luck LA. Exploring the role of amino acid-18 of the leucine binding proteins of *E. coli*. J Biomol Struct Dynam 2002;20:381–388.
8. Luck LA, Johnson C. Fluorescence and ^{19}F NMR evidence that phenylalanine, 3-L-fluorophenylalanine and 4-L-fluorophenylalanine bind to the L-leucine specific receptor of *Escherichia coli*. Protein Sci 2000;9:2573–2576.
9. O'Hara PJ, Sheppard PO, Thogersen H, Venezia D, Haldeman BA, McGrane V, Houamed KM, Thomsen C, Gilbert TL, Mulvihill ER. The ligand-binding domain in metabotropic glutamate receptors is related to bacterial periplasmic binding proteins. Neuron 1993;11: 41–52.
10. Bessis AS, Bertrand HO, Galvez T, De Colle C, Pin JP, Acher F. Three-dimensional model of the extracellular domain of the type 4a metabotropic glutamate receptor: new insights into the activation process. Protein Sci 2000;9:2200–2209.
11. Lynch DR, Guttmann RP. NMDA receptor pharmacology:perspectives from molecular biology. Curr Drug Targets 2001;2:215–231.
12. Paoletti P, Perin-Dureau F, Fayyazuddin A, Le Goff A, Callebaut I, Neyton J. Molecular organization of a zinc binding n-terminal modulatory domain in a NMDA receptor subunit. Neuron 2000;28: 911–925.
13. Adams MD, Maguire DJ, Oxender DL. Altering the binding activity and specificity of the leucine binding proteins of *Escherichia coli*. J Biol Chem 1991;266:6209–6214.
14. Salopek-Sondi B, Luck LA. ^{19}F NMR Study of the leucine specific binding protein of *E. coli*: mutagenesis and assignment of the 5-fluorotryptophane labeled residues. Protein Eng 2002;15:857–861.
15. Skeels MC. The urea induced unfolding of two reriplasmic binding proteins from Escherichia coli: the leucine-specific (LS) and leucine-isoleusine-valine (LIV) binding proteins. PhD thesis. Clarkson University, 2000.
16. Makhatadze GI. Thermodynamics of protein interactions with urea and guanidinium hydrochloride. J Phys Chem 1999;B 103: 4781–4785.
17. Pace CN. Determination and analysis of urea and guanidine hydrochloride denaturation curves. Methods Enzymol 1986;131: 266–280.
18. Santoro MM, Bolen DW. Unfolding free energy changes determined by the linear extrapolation method. 1. Unfolding of phenylmethanesulfonyl alpha chymotrypsin using different denaturants. Biochemistry 1988;27:8063–8068.
19. Eftink MR. Use of multiple spectroscopic methods to monitor equilibrium unfolding of proteins. Methods Enzymol 1995;259:487–512.
20. Olah GA, Trakhanov S, Trewhella J, Quiocho FA. Leucine/isoleucine/valine-binding protein contracts upon binding of ligand. J Biol Chem 1993;268:6241–16247.
21. Schellman J. Macromolecular binding. Biopolymers 1975;14:999–1018.
22. Brandts JF, Hu CQ, Lin LN, Mos MT. A simple model for proteins with interacting domains. Applications to scanning calorimetry data. Biochemistry 1989;28:8588–8596.
23. Wagner G, Kalb A, Wuthrich K. Conformational studies by ^{1}H NMR of the basic pancreatic trypsin inhibitor after reduction of the disulfide bond between Cys14 and Cys38. Eur J Biochem 1979;95:249–253.
24. Creighton TE. Review article on protein folding. Biochem J 1990;270:1–16.
25. Makhatadze GI, Privalov PL. Energetics of protein structure. Advan Protein Chem 1995;47:307–425.
26. Pace CN, Grimsely G, Thompson J, Barnett B. Conformational stability and activity of ribonuclease-t1 with zero, one and two intact disulfide bonds. J Mol Biol 1988;263:11820–11825.
27. Abkevich VI, Gutin AM, Shakhnovich EI. What can disulfide bonds tell us about protein energetics, function and folding: simulations and bioinformatics analysis. J Mol Biol 2000;300:975–985.
28. Sack JS, Saper MA, Quiocho FA. Periplasmic binding protein structure and function. Refined X-ray structures of the leucine/isoleucine/valine-binding protein and its complex with leucine. J Mol Biol 1989;206:171–191.
29. Sack JS, Trakhanov SD, Tsigannik IH, Quiocho FA. Structure of the L-leucine-binding protein refined at 2.4 A resolution and comparison with the Leu/Ile/Val-binding protein structure. J Mol Biol 1989;206:193–207.
30. Sayle RA, Milner-White EJ Rasmol:biomolecular graphics for all. Trends Biochem Sci 1995;20: 374–376.